

# Structural insight into the magnesium borohydride – ethylenediamine solid-state Mg-ion electrolyte system

Igor E. Golub,<sup>a</sup> Michael Heere,<sup>\*b,c</sup> Volodia Gounaris,<sup>a</sup> Xiao Li,<sup>a</sup> Timothy Steenhaut,<sup>a</sup> Jian Wang,<sup>a</sup> Koen Robeyns,<sup>a</sup> Hai-Wen Li,<sup>d</sup> Iurii Dovgaliuk,<sup>e</sup> Kazutaka Ikeda,<sup>f</sup> Geoffroy Hautier<sup>a</sup> and Yaroslav Filinchuk<sup>\*a</sup>

a. Institute of Condensed Matter and Nanosciences (IMCN), Université catholique de Louvain (UCLouvain), 1348, Louvain-la-Neuve, Belgium.

b. Institute for Applied Materials—Energy Storage Systems (IAM-ESS), Karlsruhe Institute of Technology (KIT), 76344 Eggenstein, Germany.

c. Technische Universität Braunschweig, Institute of Internal Combustion Engines, Hermann-Blenk-Straße 42, 38108 Braunschweig, Germany

d. Hefei General Machinery Research Institute (HGMRI), Hefei 230031, China

e. Swiss–Norwegian Beamlines, European Synchrotron Radiation Facility, 71 Rue des Martyrs, Grenoble, 38043, France

f. Institut des Matériaux Poreux de Paris, Ecole Normale Supérieure, ESPCI Paris, CNRS, PSL Université, 75005 Paris, France

g. Institute of Materials Structure Science, High Energy Accelerator Research Organization (KEK), Tsukuba, Ibaraki 305-0801, Japan

† E-mail: m.heere@tu-bs.de, yaroslav.filinchuk@uclouvain.be

## Electronic Supplementary Information

### Table of contents

<b>Spectroscopic characterization of the samples having <math>\text{Mg}(\text{en})_1(\text{BH}_4)_2</math> and <math>\text{Mg}(\text{en})_{1.2}(\text{BH}_4)_2</math> nominal compositions</b>	S2
<b>Figure S1.</b> ATR-FTIR spectra for the samples of the nominal compositions $\text{Mg}(\text{en})(\text{BH}_4)_2$ and $\text{Mg}(\text{en})_{1.2}(\text{BH}_4)_2$	S2
<b>Figure S2.</b> Solid state $^{11}\text{B}$ NMR spectra for the samples of the nominal compositions $\text{Mg}(\text{en})(\text{BH}_4)_2$ and $\text{Mg}(\text{en})_{1.2}(\text{BH}_4)_2$ , along with the spectrum of the precursor $\gamma\text{-Mg}(\text{BH}_4)_2$	S2
<b>Detailed description of the crystal structure of <math>\text{Mg}(\text{en})_{1.2}(\text{BH}_4)_2</math></b>	S3
<b>Table S1.</b> Geometry of dihydrogen bonds in $\text{Mg}(\text{en})_{1.2}(\text{BH}_4)_2$	S3
<b>Figure S3.</b> Crystal structure of $\text{Mg}(\text{en})_{1.2}(\text{BH}_4)_2$ with empty voids (with coordinates 0.247 0.937 0.931 and 0.375 0.166 0.752) shown in ochre	S4
<b>Characterization of the impurity phases</b>	S5
<b>Figure S4.</b> The SR-XPD of the isolated “impurity phase”, marked as I in Figure 1	S5
<b>Description of the crystal structure of <math>\text{Mg}(\text{en})_2(\text{BH}_4)_2</math></b>	S5
<b>Table S2.</b> Geometry of dihydrogen bonds in $\text{Mg}(\text{en})_2(\text{BH}_4)_2$	S5
<b>References</b>	S6

**Spectroscopic characterization of the samples having  $\text{Mg}(\text{en})_1(\text{BH}_4)_2$  and  $\text{Mg}(\text{en})_{1.2}(\text{BH}_4)_2$  nominal compositions**

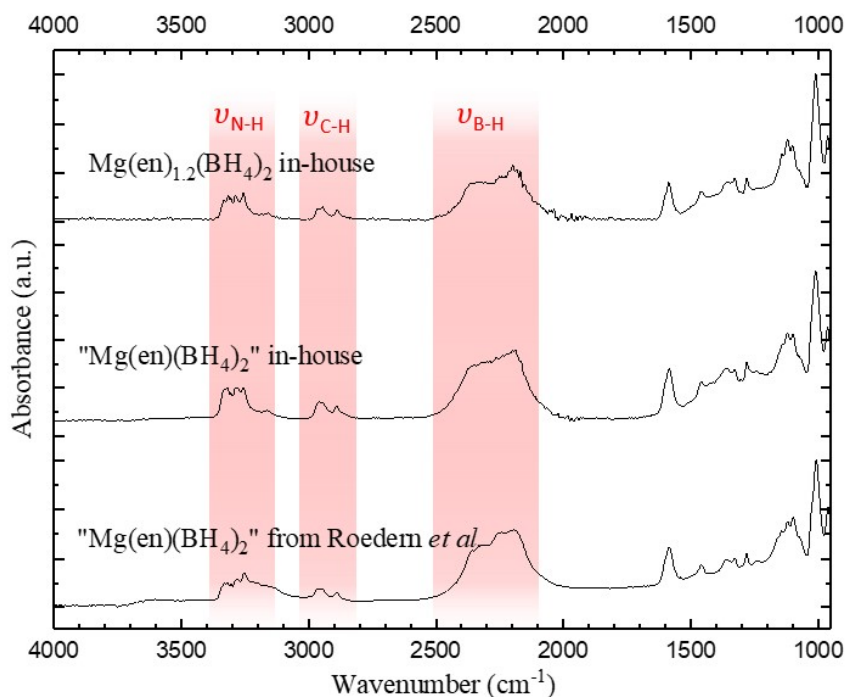


**Figure S1.** ATR-FTIR spectra for the samples of the nominal compositions  $\text{Mg}(\text{en})(\text{BH}_4)_2$  and  $\text{Mg}(\text{en})_{1.2}(\text{BH}_4)_2$ , compared to the spectrum reported in Ref. <sup>1</sup>.

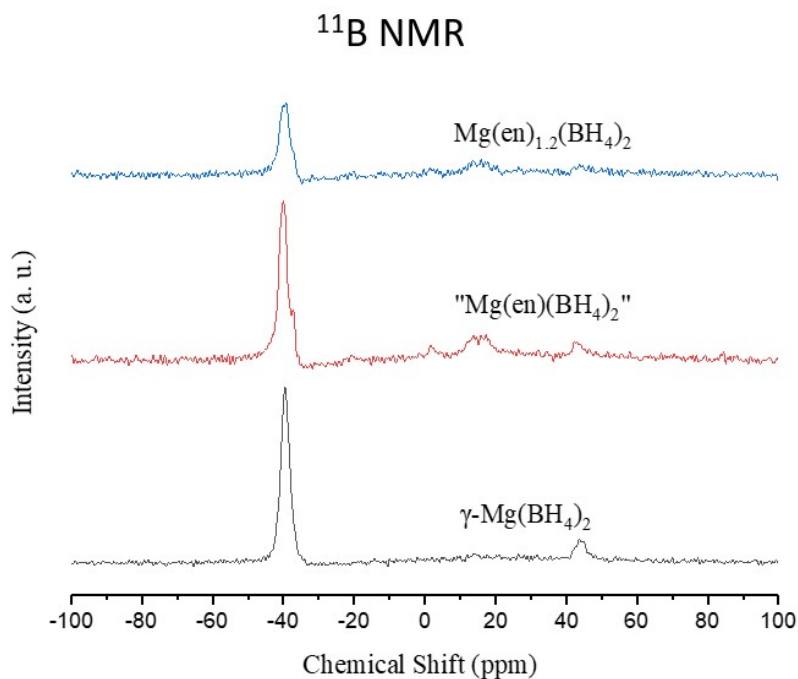


**Figure S2.** Solid state  $^{11}\text{B}$  NMR spectra for the samples of the nominal compositions  $\text{Mg}(\text{en})(\text{BH}_4)_2$  and  $\text{Mg}(\text{en})_{1.2}(\text{BH}_4)_2$ , along with the spectrum of the precursor  $\gamma\text{-Mg}(\text{BH}_4)_2$ . There are also some small peaks at 14.8 ppm and at 42.2 ppm and a bump around 14.8 ppm, we attribute them to hydrolysis products resulting from handling the samples for the NMR experiment.

## Detailed description of the crystal structure of $\text{Mg}(\text{en})_{1.2}(\text{BH}_4)_2$

The  $[\text{Mg}_3(\text{en})_5(\text{BH}_4)_4]^{2+}$  cation is constituted of the coordination polymer strands  $-\{\text{Mg}^{2+}(\kappa^2\text{-en})_2(\mu_2, \kappa^{1,2}:\kappa^2\text{-BH}_4^-)\text{Mg}^{2+}(\kappa^2\text{-en})(\kappa^2\text{-BH}_4^-)(\mu_2\text{-en})\text{Mg}^{2+}(\kappa^2\text{-en})(\kappa^2\text{-BH}_4^-)(\mu_2, \kappa^2:\kappa^{1,2}\text{-BH}_4^-)\}_-$ . The central core of the polymer strands  $[\{\text{Mg}_2(\kappa^2\text{-en})(\kappa^{1,2}\text{-BH}_4)(\kappa^2\text{-BH}_4)\}_2(\mu_2\text{-en})]$  is actually formed by two  $\text{Mg}(\text{en})_1(\text{BH}_4)_2$  fragments connected by a bridging *en*. One  $\text{BH}_4^-$  group ( $r[(\text{B})\text{H}_1\cdots\text{Mg}] = 1.99(5)$  Å,  $\angle\text{Mg}\cdots\text{H}_1\text{B} = 102(3)^\circ$ ;  $r[(\text{B})\text{H}_2\cdots\text{Mg}] = 2.10(5)$  Å,  $\angle\text{Mg}\cdots\text{H}_2\text{B} = 96(3)^\circ$ ;  $r[\text{B}\cdots\text{Mg}] = 2.497(9)$  Å) has an asymmetric bidentate coordination mode ( $\kappa^2$ ). Another  $\text{BH}_4^-$  group serve as bridging ligand between neutral  $[\{\text{Mg}_2(\kappa^2\text{-en})(\kappa^{1,2}\text{-BH}_4)(\kappa^2\text{-BH}_4)\}_2(\mu_2\text{-en})]$  fragment and cationic  $[\text{Mg}(\kappa^2\text{-en})_2]^{2+}$  fragment lead to  $[\text{Mg}_3(\text{en})_5(\text{BH}_4)_4]^{2+}$  complex cation formation. It has bidentate coordination ( $\kappa^2$ ) to one Mg atom in the central neutral core ( $r[(\text{B})\text{H}_1\cdots\text{Mg}] = 2.04(5)$  Å,  $\angle\text{Mg}\cdots\text{H}_1\text{B} = 100(3)^\circ$ ;  $r[(\text{B})\text{H}_2\cdots\text{Mg}] = 2.07(5)$  Å,  $\angle\text{Mg}\cdots\text{H}_2\text{B} = 99(3)^\circ$ ;  $r[\text{B}\cdots\text{Mg}] = 2.49(1)$  Å) and mixed coordination mode ( $\kappa^{1,2}$ )<sup>2, 3</sup> to Mg in cationic fragment ( $r[(\text{B})\text{H}_1\cdots\text{Mg}] = 2.28(6)$  Å,  $\angle\text{Mg}\cdots\text{H}_1\text{B} = 107^\circ$ ;  $r[(\text{B})\text{H}_2\cdots\text{Mg}] = 2.46(6)$  Å,  $\angle\text{Mg}\cdots\text{H}_2\text{B} = 96^\circ$ ;  $r[\text{B}\cdots\text{Mg}] = 2.809(10)$  Å). These distances are farther than what is usually encountered in the literature with  $r[(\text{B})\text{H}\cdots\text{Mg}] = 2.01\text{--}2.12$  Å and  $r[\text{B}\cdots\text{Mg}] = 2.39\text{--}2.45$  Å.<sup>4</sup>

The  $[\{\text{Mg}(\kappa^3\text{-BH}_4)(\kappa^2\text{-BH}_4)_2\}_2(\mu_2\text{-en})]^{2-}$  anion is constituted of two  $[\text{Mg}(\text{BH}_4)_3]^-$  fragments connected by a bridging *en*. One  $\text{BH}_4^-$  group connected to each Mg atom ( $r[(\text{B})\text{H}_1\cdots\text{Mg}] = 2.12(5)$  Å,  $\angle\text{Mg}\cdots\text{H}_1\text{B} = 82(2)^\circ$ ;  $r[(\text{B})\text{H}_2\cdots\text{Mg}] = 2.15(5)$  Å,  $\angle\text{Mg}\cdots\text{H}_2\text{B} = 81(3)^\circ$ ;  $r[(\text{B})\text{H}_3\cdots\text{Mg}] = 2.22(5)$  Å,  $\angle\text{Mg}\cdots\text{H}_3\text{B} = 78(2)^\circ$ ;  $r[\text{B}\cdots\text{Mg}] = 2.276(9)$  Å) has tridentate coordination mode ( $\kappa^3$ ). Another two  $\text{BH}_4^-$  groups ( $r[(\text{B})\text{H}_1\cdots\text{Mg}] = 2.01(4)$  Å,  $\angle\text{Mg}\cdots\text{H}_1\text{B} = 99(3)^\circ$ ;  $r[(\text{B})\text{H}_2\cdots\text{Mg}] = 2.01(5)$  Å,  $\angle\text{Mg}\cdots\text{H}_2\text{B} = 99(3)^\circ$ ;  $r[\text{B}\cdots\text{Mg}] = 2.434(8)$  Å and  $r[(\text{B})\text{H}_1\cdots\text{Mg}] = 1.99(5)$  Å,  $\angle\text{Mg}\cdots\text{H}_1\text{B} = 100(3)^\circ$ ;  $r[(\text{B})\text{H}_2\cdots\text{Mg}] = 2.06(5)$  Å,  $\angle\text{Mg}\cdots\text{H}_2\text{B} = 96(3)^\circ$ ;  $r[\text{B}\cdots\text{Mg}] = 2.437(8)$  Å) have bidentate coordination mode ( $\kappa^2$ ).

Crystal structure of  $\text{Mg}(\text{en})_{1.2}(\text{BH}_4)_2$  is also stabilized due to formation network of monodentate and bifurcate (B)H $\cdots$ H(N) dihydrogen bonds<sup>5-8</sup> with  $r(\text{H}\cdots\text{H})$  distances 2.04–2.36 Å (that less than sum of van der Waals radii for two H atoms,  $\sum r_{\text{vdw}}(\text{H}\text{--}\text{H}) = 2.4$  Å) and  $\angle\text{NH}\cdots\text{H}(\text{B}) = 136\text{--}171^\circ$  and  $\angle\text{BH}\cdots\text{H}(\text{N}) = 91\text{--}108^\circ$  (Table S1). Dihydrogen bonds are responsible for the additional adhesion force within the cation, anion, and between them.

**Table S1.** Geometry of dihydrogen bonds in  $\text{Mg}(\text{en})_{1.2}(\text{BH}_4)_2$ .

(N)H	H(B)	$r[\text{H}\cdots\text{H}]$ , Å	$\angle\text{NH}\cdots\text{H}(\text{B})$ , °	$\angle(\text{N})\text{H}\cdots\text{HB}$ , °	Localisation
H15A	H18D	2.04	171	107	
H15A	H18C	2.34	138	91	Within cation
H12B	H24C	2.19	136	108	
H22A	H18B	2.11	148	105	
H22A	H18D	2.36	162	92	Cation-anion
H22B	H25C	2.28	143	99	
H22B	H25D	2.23	162	103	Within anion

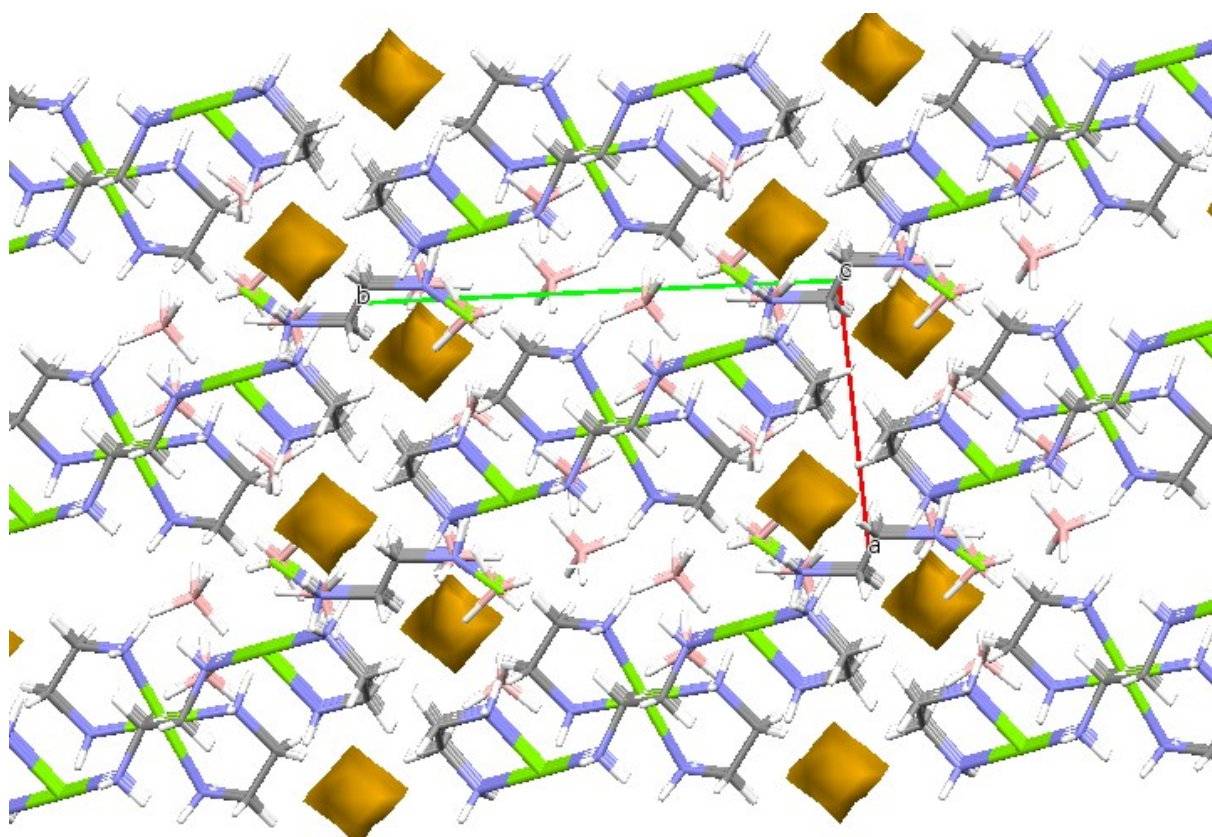


**Figure S3.** Crystal structure of  $\text{Mg}(\text{en})_{1.2}(\text{BH}_4)_2$  with empty voids (with coordinates 0.247 0.937 0.931 and 0.375 0.166 0.752) shown in ochre.

## Characterization of the impurity phases

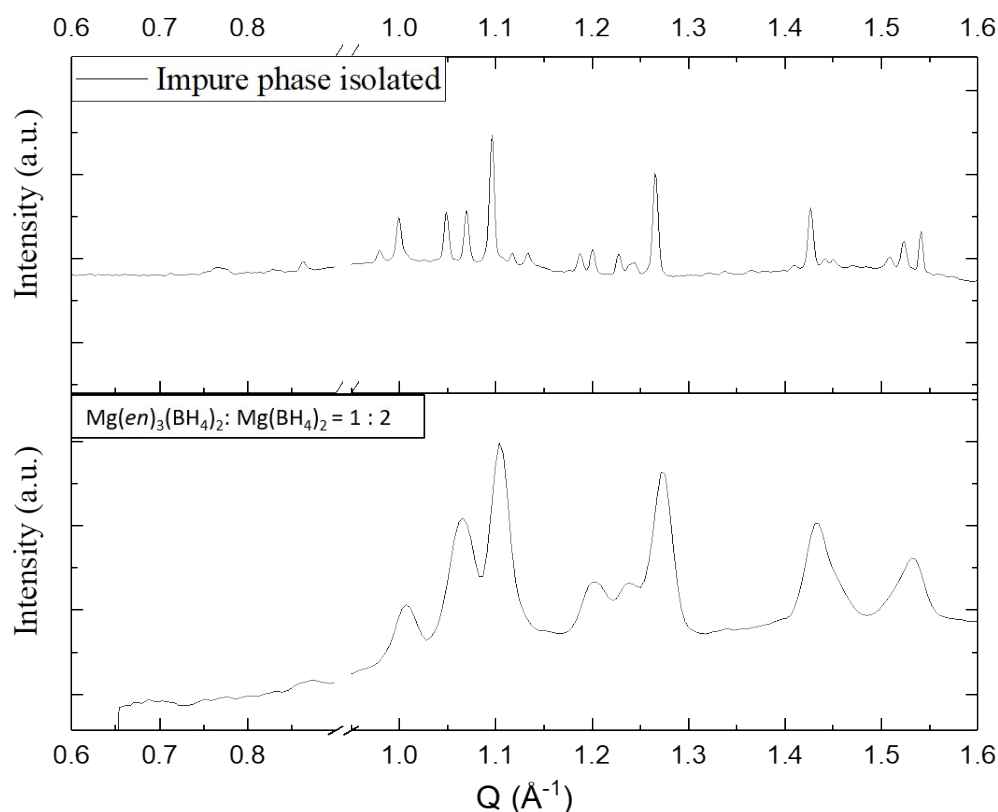


**Figure S4.** The SR-XPD of the isolated “impurity phase”, marked as I in Figure 1.

### Description of the crystal structure of $\text{Mg}(\text{en})_2(\text{BH}_4)_2$

The crystal structure of  $\text{Mg}(\text{en})_2(\text{BH}_4)_2$  is displayed in Figure 5. It is composed of  $[\text{Mg}(\kappa^2\text{-en})_2(\kappa^2\text{-BH}_4)]^+$  cations and  $\text{BH}_4^-$  anions. One  $\text{BH}_4^-$  is coordinated to Mg atom ( $r[(\text{B})\text{H}\cdots\text{Mg}] = 2.06 \text{ \AA}$ ,  $\angle\text{Mg}\cdots\text{HB} = 92^\circ$ ;  $r[\text{B}\cdots\text{Mg}] = 2.458 \text{ \AA}$ ) in a bidentate manner ( $\kappa^2$ ). Another  $\text{BH}_4^-$  anion is not coordinated to the metal atom, but it is linked by a series of dihydrogen bonds<sup>6, 9</sup>:  $r(\text{H}\cdots\text{H})$  distances  $1.97\text{--}2.28 \text{ \AA}$  and  $\angle\text{NH}\cdots\text{H}(\text{B}) = 134\text{--}160^\circ$  and  $\angle\text{BH}\cdots\text{H}(\text{N}) = 95\text{--}108^\circ$  (Table S2).

**Table S2.** Geometry of dihydrogen bonds in  $\text{Mg}(\text{en})_2(\text{BH}_4)_2$ .

(N)H	H(B)	$r[\text{H}\cdots\text{H}], \text{ \AA}$	$\angle\text{NH}\cdots\text{H}(\text{B}), ^\circ$	$\angle(\text{N})\text{H}\cdots\text{H}(\text{B}), ^\circ$
H12	H2	1.97	136	108
H11	H2	2.15	135	101
H11	H1	2.28	160	99
H9	H2	2.28	134	95



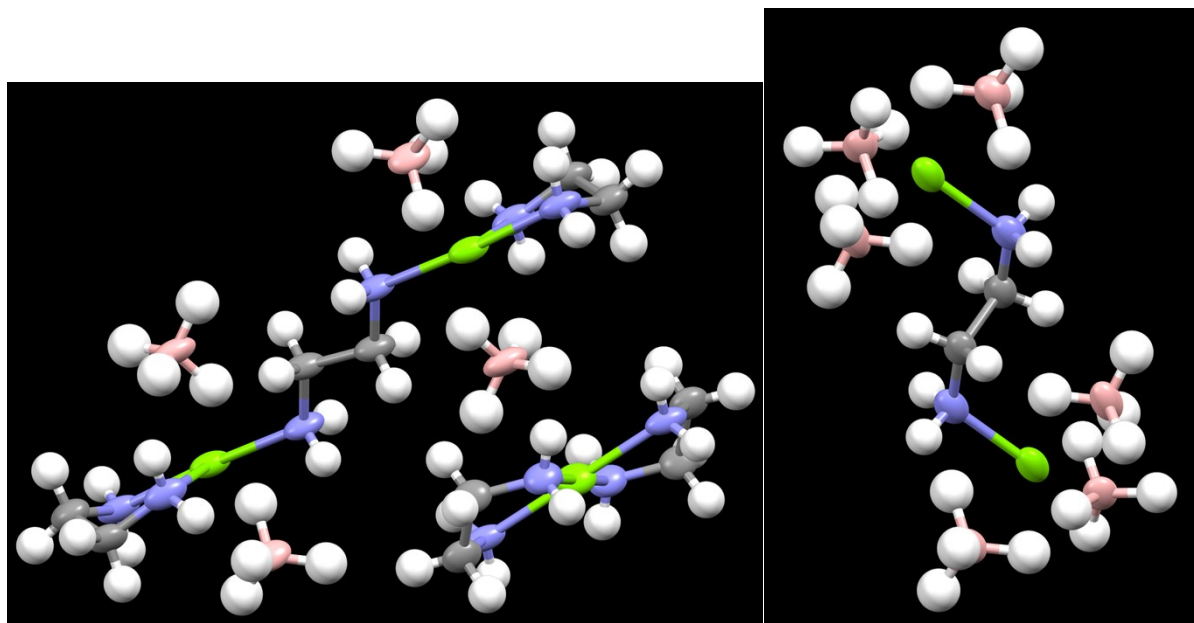


**Figure S5.** Fragments of the crystal structure of  $\text{Mg}(\text{en})_{1.2}(\text{BH}_4)_2$  showing ADPs as 50% probability ellipsoids.

## References

1. E. Roedern, R.-S. Kühnel, A. Remhof and C. Battaglia, *Sci. Rep.*, 2017, **7**, 46189.
2. S. V. Safronov, E. S. Osipova, Y. V. Nelyubina, O. A. Filippov, I. G. Barakovskaya, N. V. Belkova and E. S. Shubina, *Molecules*, 2020, **25**.
3. S. V. Safronov, E. I. Gutsul, I. E. Golub, F. M. Dolgushin, Y. V. Nelubina, O. A. Filippov, L. M. Epstein, A. S. Peregudov, N. V. Belkova and E. S. Shubina, *Dalton Trans.*, 2019, **48**, 12720-12729.
4. Y. Filinchuk, D. Chernyshov and V. Dmitriev, in *Boron hydrides, high potential hydrogen storage material*, eds. U. B. Demirci and P. Miele, Nova Publishers, 2010, pp. 137-164.
5. O. A. Filippov, N. V. Belkova, L. M. Epstein and E. S. Shubina, *J. Organomet. Chem.*, 2013, **747**, 30-42.
6. V. I. Bakhmutov, *Dihydrogen Bonds: Principles, Experiments, and Applications*, John Wiley & Sons, Inc., Hoboken, New Jersey, 2008.
7. R. Custelcean and J. E. Jackson, *Chem. Rev. (Washington, DC, U. S.)*, 2001, **101**, 1963-1980.
8. W. T. Klooster, T. F. Koetzle, P. E. M. Siegbahn, T. B. Richardson and R. H. Crabtree, *J. Am. Chem. Soc.*, 1999, **121**, 6337-6343.
9. N. V. Belkova, L. M. Epstein, O. A. Filippov and E. S. Shubina, *Chem. Rev. (Washington, DC, U. S.)*, 2016, **116**, 8545-8587.